In-situ/operando X-ray absorption spectroscopy for energy science at beamline 7.3.1 of the ALS

Feipeng Yang[#1], Yi-Sheng Liu[#1], Xuefei Feng[#1], Per-Anders Glans[1], James Nasiatka[1], Dmitriy Voronov[1], Jun Feng[2], Yi-De Chuang[1], Howard Padmore[1], Jinghua Guo[1]

[1]Advanced Light source, Lawrence Berkeley National Laboratory, Berkeley, California 94720, United States

[2]Department of Materials Science and Engineering, Institute for Quantum Science and Engineering, South University of Science and Technology, Shenzhen 518055, Guangdong, P.R. China

♯: equal contribution

■要旨

The new endstation at the bending magnet beamline 7.3.1 of the Advanced Light Source (ALS), Lawrence Berkeley National Laboratory (LBNL), has been commissioned and is open for general user operation. The beamline is repurposed from the previous photoemission electron microscopy (PEEM) to X-ray absorption spectroscopy (XAS) with in-situ/operando capabilities. The simplest optical scheme that combines a spherical grating monochromator and a downstream horizontal focusing mirror maximizes the incident photon flux at this beamline. The endstation integrated with in-situ/operando capabilities will fulfill the increasing demand for XAS technique, benefiting not only the discovery of new materials but also the synergy across different fields of discipline. The details of the beamline and endstation designs and their performance are presented in this article.

1. Introduction

Synchrotron-based X-ray absorption spectroscopy (XAS), which measures the X-ray absorption coefficient as a function of incident photon energy, is a probe sensitive to the oxidation state, bond length, and coordination chemistry for various materials, including solid, liquid, and gas.[1,2] Since the early 1990s, XAS has been a well-developed, extremely powerful tool for routine studies of the electronic structure of target samples with elemental and chemical sensitivity.[3–5] The demand for accessing synchrotron-based XAS spectroscopy has been growing steadily as a result of advanced material synthesis methods and prompt material discovery, especially in energy science and catalysis research. For example, XAS has been deployed in the studies of graphene oxide wrapped magnesium complex for hydrogen storage, Cu nanoparticle catalysts for CO_2 reduction, SnO_x/Pt-Cu-Ni heterojunction catalyst for ORR, and lithium 3*d* transition metal oxide battery materials.[6–11] Additionally, the tremendous efforts in improving the material stability and performance by doping[12], nanoscaling[13–15], encapsulation[16], and hybridization in the metal-organic framework (MOF)[17–19], to name a few, often require XAS as a characterization tool to evaluate the chemical property at the microscopic level and guide the next-stage sample modifications. Consequently, this simple but important technique is in high demand in synchrotron facilities worldwide.

At the Advanced Light Source (ALS), the beamtime proposals for soft X-ray XAS at beamline 8.0.1 are competing with others that request novel spectroscopy such as the resonant inelastic X-ray scattering (RIXS)[20,21] at the same beamline. As a result, this beamline is heavily oversubscribed and only a small fraction of the huge demand for time-consuming in-situ/operando XAS measurements can be met. To mitigate this beamtime bottleneck, developing a new endstation dedicated for soft XAS at a different beamline is inevitable. In addition, this endstation can also facilitate the material discovery with the aid of machine learning[22] in the future.

The new endstation is located at beamline 7.3.1, which is repurposed from the previous photoemission electron microscopy (PEEM) beamline. Since its operation, it has significantly alleviated the oversubscription of beamline 8.0.1 for XAS studies. This endstation is actively used in the characterization of critical samples from the Hydrogen Materials Advanced Research Consortium (HyMARC) for hydrogen storage, Joint Center for Energy Storage Research (JCESR) for battery research, and Liquid Sunlight Alliance (LiSA) for liquid sunlight, artificial photosynthesis. Its in-situ/operando capability enables the probing of transient species, such as those at the battery working electrode/electrolyte interfaces.[1,23–26]

The designed photon energy range for this endstation is from 250 eV (carbon K-edge) to 1650 eV (aluminum K-edge), covering the K-edge of light elements and L-edge of $3d$ transition metals. It allows a detailed and high-statistic detection of the $1s$-$2p$ and $2p$-$3d$ transitions, ideal for the study of electrochemical operando battery materials which usually involve the $3d$ transition metals. The high energy end that reaches the magnesium (1320 eV) and Al (1570 eV) K-edge is very useful because these elements play a critical role in multivalent batteries and catalysis, respectively, and there are only a handful of beamlines worldwide that can cover this energy range across the synchrotron light sources worldwide in spite of the fact that magnesium and aluminum are becoming critical in multivalent batteries[27,28] and catalysis[29], respectively. The endstation has two chambers that are in series. The first chamber is dedicated for the ultra-high vacuum (UHV) solid-state XAS measurement and the second chamber is for the in-situ measurements. There is a safety interlock between these two chambers in case of vacuum failure during the in-situ/operando measurements.

2. Design

2.1 Beamline

The idea with beamline 7.3.1 was to make a system with a minimum number of reflections, giving the smallest horizontal focus. In the original design, the focal plane was at the sample surface for a PEEM, and the field of view (30 μm) of the PEEM effectively acted as a vertical exit slit. An elliptical mirror focused in the horizontal direction at high demagnification, matching the horizontal to the vertical field sizes. The very small vertical source size allows the use of a very low line density (200 l/mm) and this limits the defocus aberration that is normally present in the spherical grating monochromator (SGM) design. In this way, longitudinally moveable exit slits do not have to be used, to move to the zero-defocus position. The detailed schematic layout of beamline 7.3.1 is shown in **Fig. 1**. The optical design uses an SGM followed by a downstream elliptical horizontal focus mirror (M1) and a fixed piezo-driven exit slit system near the endstation. This optical design minimizes the number of optical elements to maximize the photon flux on the sample. The CAD drawing of the internal components of the monochromator is shown in **Fig. 2**. The grating substrate is held in a cradle by two cross-bars under light compression using wave springs. This keeps the grating secure, without applying enough clamping force to distort the optical surface. Thermal stability is achieved by water cooling using a pair of trapezoidal shaped bars with a thin layer of liquid eutectic Indium/Gal-

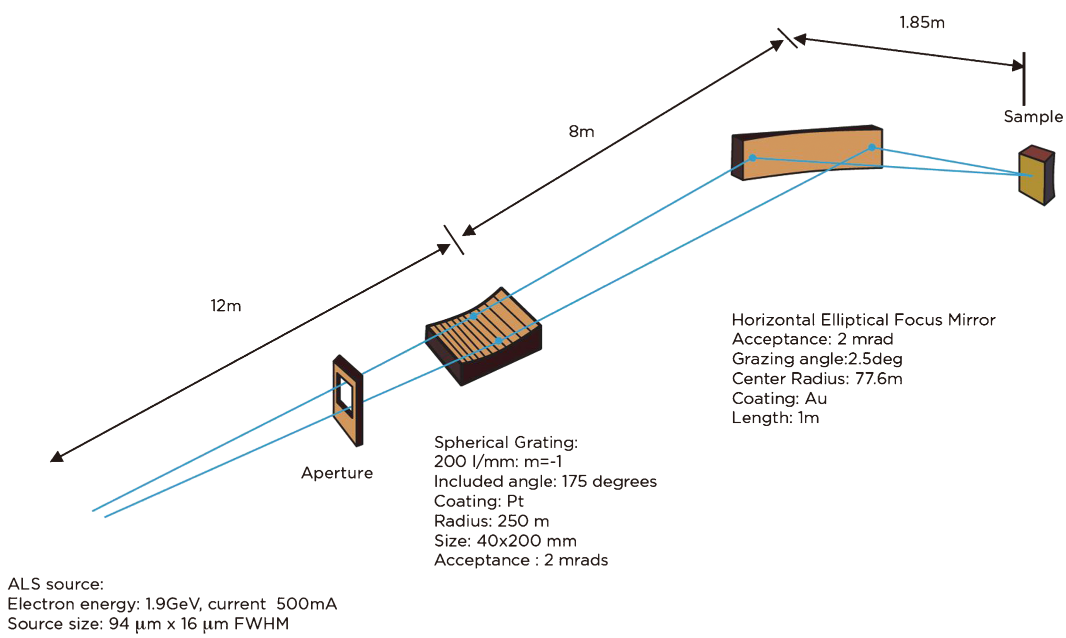

Fig. 1 (Color online) Beamline 7.3.1 overview.

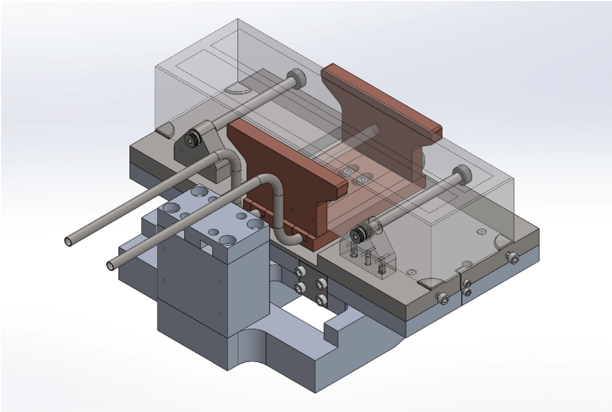

Fig. 2 (Color online) Beamline monochromator support and design.

lium (eGaIn) to provide thermal contact with the substrate. This allows for efficient thermal transfer without applying any stress on the substrate from both clamping forces and thermal expansion of the grating. The trapezoidal shape allows for optimizing the cooling along the length of the grating to minimize any thermal deformation and slope errors.

The mounting cradle is attached to a central shaft that rotates about the grating axis using a high-precision stage and sine-bar assembly. The sine-bar is affixed to the stage using a ball and vee-groove mounting with spring loading allowing for smooth rotation of the bar while allowing for small amounts of translation at the attachment point. The cooling lines run down the center of this shaft and use a novel modified VCR feedthrough design that allows for a single cooling line with no breaks, eliminating the need for any air guarding. The rotation shaft and sine-bar assembly are all mounted on a translation platform that moves the monochromator between the two grating settings. The monochromator assembly is fixed to an epoxy-granite mounting base that provides thermal and vibrational stability. There are two gratings in the monochromator. These gratings, ruled on a single silicon substrate, have a 230 mm × 26 mm ruled area and are separated by 6 mm laterally. They have the same line density (200 l/mm) but different groove depths to cover disparate photon energy ranges. The grating with 14 nm and 7 nm groove depth covers 250-750 eV and 500-1500 eV, respectively.

A grating carriage that houses these two gratings is mounted on a motorized linear translator that moves the gratings across the beam path. A motorized sine-arm with an optical encoder on the motor shaft drives the grating angle to change the incident photon energy. The design of the

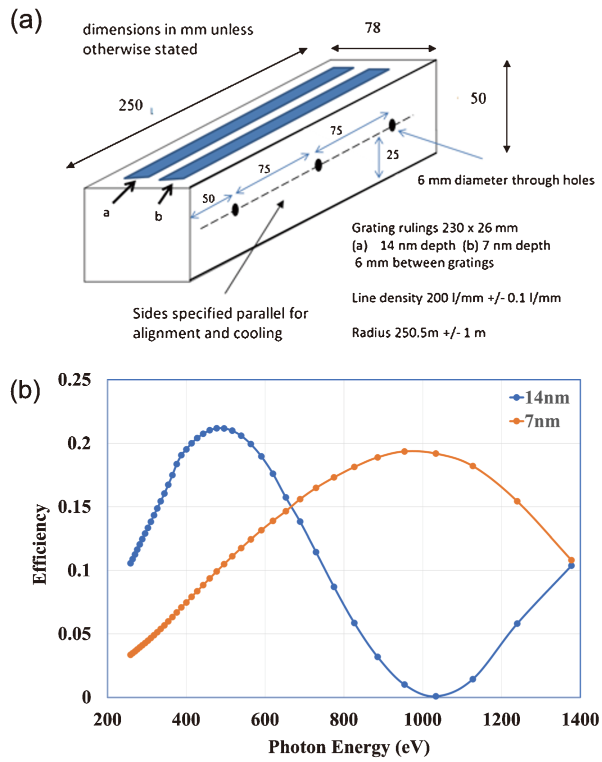

Fig. 3 (Color online) (a) Dimensions of the monochromator and (b) the grating efficiency vs. photon energy (eV) on the monochromator with a ruling depth of 14 nm or 7 nm.

sine arm allows the fast and stable angular scan for quick XAS measurements. The dimensions of the monochromator and the calculated grating efficiency are shown in **Fig. 3**. The efficiency of the grating with 14 nm and 7 nm groove depth is optimized at 470 eV and 920 eV, respectively. Therefore, they can be regarded as high- and low-energy grating, respectively. The angular motion of the monochromator for selecting monochromatic light is driven by an external sine bar (lever), for which the angle is calculated from the sine bar movement projecting in the vertical direction with hardware limit switches (as shown in **Fig. 2**). This design offers the angular (energy) scan in a fast, stable, and relatively simple fashion.

The downstream elliptical horizontal focusing mirror, which is 1 m in length, focuses the beam horizontally near the exit slit location. The beam size and the transmitted spectral bandwidth are controlled by the four-piezo slit system shown in **Fig. 4**.

Thus 7.3.1 is the simplest possible configuration, with the highest throughput of any optical configuration. It should be noted that in the case of the ALS upgrade, ALS-U, the horizontal object size will be five times smaller,

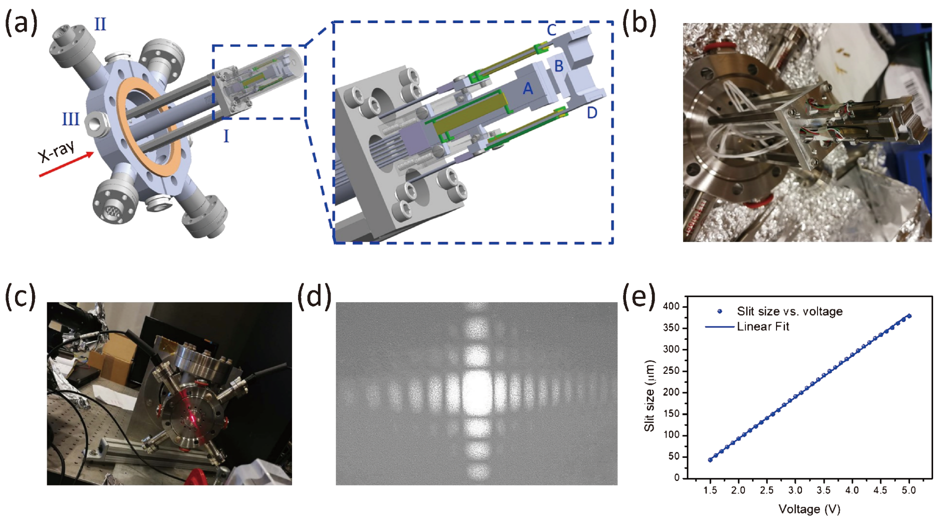

Fig. 4 (Color online) (a) 3D model of the piezo slit and the enlarged image of the slit assembly. (b) The photo of the slit without cover. (c) Set up of the system for slit size measurement. (d) Single slit diffraction image with 2 V applied on the slit and 5 V applied on the horizontal aperture. (e) Exit slit size as a function of applied voltage. The experimental data and linear fitted curve are shown as the round blue circles and blue line, respectively.

and so for the same image size, a new horizontally focusing mirror can have an image distance about five times larger than at present and collect five times the aperture. Due to these features, with a design optimized for ALS-U, undulator-like photon flux densities can be achieved at the sample. The general idea was to make a system that was as low in cost as possible, but maintaining very high photon flux density, so that in principle it could be replicated to expand the scientific program.

2.2 Piezo exit slit

Unlike most soft X-ray beamlines, the exit slit of the monochromator is 20 mm upstream from the sample location in the first chamber. Limited by the available space, the traditional design of exit slit that comprises a motorized two-knife-edge assembly for SGM cannot be used. To resolve this issue, a compact slit assembly was designed, and the CAD model is shown in **Fig. 4(a)**. The assembly mounted on a special 4.5” CF flange contains three parts labeled I, II, and III. The photograph of the slit assembly is shown in **Fig. 4(b)**.

Part I is the main component of the slit assembly. It has the piezo bending actuators with position sensors. The control units are from Physik Instruments (PI) GmbH & Co. KG. Four aluminum knife-edges marked A-D in the figure are mounted on the tip of the piezo bending actuators. Their positions can be changed by applying voltages on the piezo benders, allowing one to precisely adjust the gap between the knife-edges. Parallel blades A and B form the horizontal aperture, which is used to limit the horizontal beamwidth on the sample. During the normal operation, the voltage applied on aperture A-B pair is +5 V, corresponding to the ~700 μm opening. The parallel blades C and D form the vertical aperture and they are used as the exit slit for the monochromator. When the voltage across the C-D pair is 0 V, the aperture is fully closed. The opening of the exit slit versus piezo driving voltage is calibrated by the optical setup, see **Fig. 4(c)**. A 650-nm laser is used to illuminate the slits to produce a diffraction pattern on a screen 940 mm away from the slit assembly [**Fig. 4(d)**]. The edges of the diffraction pattern are parallel to each other, indicating a good parallelism and alignment of the blades. By adjusting the piezo driving voltage and determining the position of the diffraction fringes, we obtain the relationship between the slit size and the voltage, which is summarized in **Fig. 4(e)**. As can be seen from this figure, the slit size varies linearly with the applied voltage in the following way:

$$\mathit{Slit\ size}\ (\mu\mathrm{m}) = 96.73 \times \mathit{Voltage}\ (\mathrm{V}) - 100.27 \qquad (1)$$

With full +5 V, the full opening of the exit slit will be 383 μm. The repeatability of the slit size has been tested and the stability is longer than three weeks.

Part II is the electric feedthrough for the piezo actuators. These feedthroughs are connected to the E-651 piezo amplifier and high precision power supply units. Part III are the fiducial monuments. They are used to set the perpendicularity for apertures A-B and C-D and the parallelism between blades in each aperture.

2.3 Experimental Endstations

The endstation consists of two experimental chambers. The first chamber (upstream) is dedicated for the UHV solid-state XAS measurements. It is equipped with a cryostat with two sample stages, which can host 20-30 samples simultaneously. The conventional XAS detection modes include the total electron yield (TEY, sample-to-ground current), total fluorescence yield (TFY, channeltron multiplier), and partial fluorescence yield (PFY, silicon drift detector) modes. For this UHV solid-state XAS chamber at beamline 7.3.1, a channeltron multiplier and a sample-to-ground current amplifier was used to collect TFY and TEY signals, respectively. The upper sample stage has two internal electrical contacts for connecting the reference and counter electrodes in the static liquid cell, whose details were reported previously.[30] We also developed a vacuum suitcase for transferring air-sensitive samples from Ar-filled glovebox to the load-lock chamber of this experimental chamber without exposure to the air. This suitcase can also be used in other endstations at beamline 8.0.1, allowing users to perform multiple spectroscopic measurements on the same samples.

The second chamber downstream of the UHV chamber is designed for the in-situ UHV XAS experiment. It can also accommodate the high pressure (10^{-5} Torr) liquid jet experiment setup. However, the second chamber is still under development due to the ongoing design of a safety interlock system. The endstation is to be an automated beamline in the next few years to maximize its XAS throughput to satisfy the growing demand from user groups.

3. XAS spectra measured at beamline 7.3.1

The operation energy range for beamline 7.3.1 is from 250 eV to 1650 eV, which covers the absorption edges from carbon to aluminum *K*-edges, and calcium to zinc *L*-edges. The energy resolution of the beamline is limited by the piezo exit slit system. The low energy grating has its efficiency optimized at the titanium *L*-edge (450 eV), where the grating parameters also give the best spectral resolving power around 6,000. The energy resolution will deteriorate progressively with increasing or decreasing the incident photon energy away from this energy. This is expected as the exit slit is stationary and will not be able to compensate for the aberrations when the grating does not fulfill the Rowland condition.

In **Fig. 5(a)**, we show the titanium *L*-edge XAS spectrum in TEY mode from TiO_2 powder (black curve). The spectrum is overlaid with that from beamline 8.0.1 (red curve). In this figure, one can see the salient spin-orbit splitting (L_2 and L_3 edge) features from unoccupied Ti t_{2g} and e_g orbitals. The observation of two weaker pre-peaks around 457 eV and the agreement to the spectrum recorded at beamline 8.0.1 substantiate the claim of high spectral resolution at this photon energy.

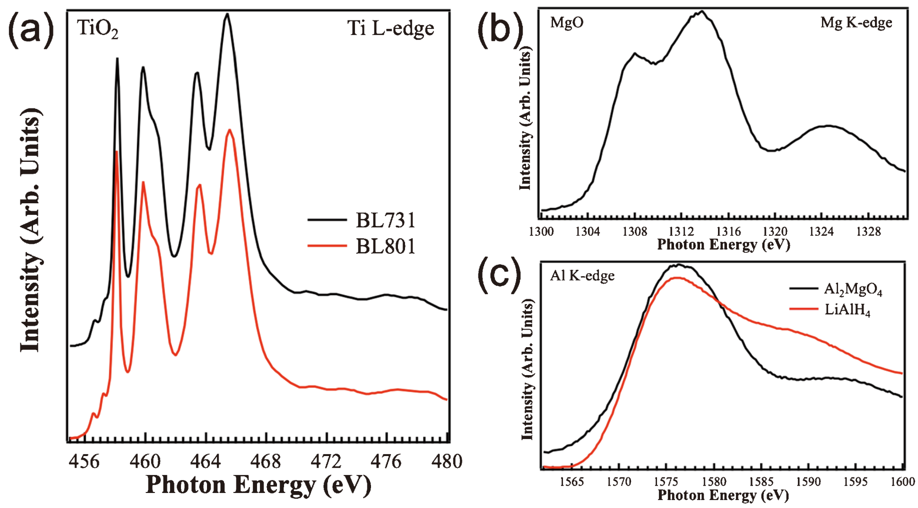

Fig. 5 (Color online) (a) High-resolution Ti *L*-edge TEY XAS spectra measured at beamline 7.3.1 and beamline 8.0.1. (b) Magnesium *K*-edge XAS spectrum and (c) Aluminum *K*-edge XAS spectra of spinel and lithium aluminum hydride.

The goal of developing this endstation is to increase the XAS capacity at the ALS, and one of the key metrics is the acquisition time for one good-statistics spectrum. With optimized photon flux from beamline 7.3.1, we can record one 25-eV wide XAS spectrum at Ti L-edge in 6 minutes if using 0.1 eV energy step and 1 second acquisition time per step. This acquisition time is actually shorter than what is needed for a comparable measurement at beamline 8.0.1 due to the fast monochromator grating scanning mechanism. In **Figs. 5(b)** and **5(c)**, we show the Mg and Al K-edge XAS spectra from MgO, Al_2MgO_4, and $LiAlH_4$, respectively. Although the energy resolution degrades when reaching these higher photon energies, the moderate energy resolution still allows us to resolve XAS features in these compounds. Additionally, the broadening of spectral features in magnesium and aluminum K-edge XAS may not be a big constraint if one wishes to differentiate gross spectral evolution with sample modifications.[31)]

4. Summary

The new endstation at ALS beamline 7.3.1 dedicated for soft X-ray absorption spectroscopy with in-situ/operando capability is now open for general user operation. The relatively simple optical design optimizes the incident photon flux and spectral resolution for performing routine XAS measurements at this bending magnet beamline. The extended high photon energy end to reach the aluminum K-edge is beneficial for energy materials and catalysis research. We show selected XAS spectra at Ti L-edge and Mg and Al K-edge to validate the designed 6,000 and 3,000 resolving power, respectively. In addition, comparison spectra with the neighboring undulator beamline 8.0.1 are provided with comparable data quality and resolution. The outcomes from the endstation are productive and increasing volumes of inquiries are received from many external user groups, including those for in-situ/operando XAS measurements.

Acknowledgement

The authors acknowledge financial support through the Hydrogen Storage Materials Advanced Research Consortium (HyMARC) of the U.S. Department of Energy (DOE), Office of Energy Efficiency and Renewable Energy, Fuel Cell Technologies Office under Contracts DE-AC52-07NA27344. This work is also supported by Director, Office of Science, Office of Basic Energy Sciences, of the U.S. DOE under Contract DE-AC02–05CH11231. This work was supported as part of the Joint Center for Energy Storage Research (JCESR), an energy innovation hub funded by the U.S. DOE. This research used resources of the Advanced Light Source, a U.S. DOE Office of Science User Facility under contract no. DE-AC02-05CH11231.

References

1) F. Yang *et al.*: Energy Environ. Mater. **4**, 139 (2021).
2) F. Lin *et al.*: Chem. Rev. **117**, 13123 (2017).
3) F. M. F. de Groot *et al.*: Phys. Rev. B **40**, 5715 (1989).
4) F. M. F. de Groot, J. C. Fuggle, B. T. Thole and G. A. Sawatzky: Phys. Rev. B **41**, 928 (1990).
5) F. M. F. de Groot, J. C. Fuggle, B. T. Thole and G. A. Sawatzky: Phys. Rev. B **42**, 5459 (1990).
6) D. Kim, C. S. Kley, Y. Li and P. Yang: Proc. Natl. Acad. Sci. U.S.A. **114**, 10560 (2017).
7) E. S. Cho *et al.*: Nat. Commun. **7**, 10804 (2016).
8) X. Shen *et al.*: J. Am. Chem. Soc. **141**, 9463 (2019).
9) J. B. Goodenough and K.-S. Park: J. Am. Chem. Soc. **135**, 1167 (2013).
10) X. Wang *et al.*: Nat. Energy **5**, 478 (2020).
11) Z. Zhao *et al.*: Matter **3**, 1774 (2020).
12) D. J. Norris, A. L. Efros and S. C. Erwin: Science **319**, 1776 (2008).
13) J. Lu *et al.*: Nat. Nanotechnol. **11**, 1031 (2016).
14) X. Fu *et al.*: Mater. Today Phys. **19**, 100418 (2021).
15) Z. Zhang *et al.*: Proc. Natl. Acad. Sci. U.S.A. **117**, 29442 (2020).
16) E. S. Cho *et al.*: Adv. Funct. Mater. **27**, 1704316 (2017).
17) A. Aijaz and Q. Xu: J. Phys. Chem. Lett. **5**, 1400 (2014).
18) W. Huang *et al.*: ACS Sustain. Chem. Eng. **5**, 5039 (2017).
19) A. Schneemann *et al.*: ACS Nano. **14**, 10294 (2020).
20) R. Qiao *et al.*: Rev. Sci. Instrum. **88**, 033106 (2017).
21) Y.-D. Chuang *et al.*: J. Synchrotron Rad. **27**, 695 (2020).
22) G. Brunin, F. Ricci, V.-A. Ha, G.-M. Rignanese and G. Hautier: NPJ Comput. Mater. **5**, 63 (2019).
23) F. Yang, X. Feng, Y.-S. Liu, P.-A. Glans and J. Guo: MRS Bull. (2021), doi:10.1557/s43577-021-00155-8.
24) L. C. Kao *et al.*: Surf. Sci. **702**, 121720 (2020).
25) F. Yang *et al.*: RSC Adv. **10**, 27315 (2020).
26) Y.-S. Liu *et al.*: Chemphyschem **20**, 1261 (2019).
27) T. S. Arthur *et al.*: ACS Appl. Mater. Interfaces **6**, 7004 (2014).
28) Y. Orikasa *et al.*: Sci. Rep. **4**, 5622 (2014).
29) C. J. Whiteoak *et al.*: J. Am. Chem. Soc. **135**, 1228 (2013).
30) Y.-S. Liu, P.-A. Glans, C.-H. Chuang, M. Kapilashrami and J. Guo: J. Electron Spectros. Relat. Phenomena **200**, 282 (2015).
31) W. Guo *et al.*: Matter **4**, 2902 (2021).

Introduction of Authors

Feipeng Yang
Advanced Light Source, Lawrence Berkeley National Laboratory
E-mail: feipeng_yang@lbl.gov
Research interests: Soft X-ray Spectroscopy, X-ray and Neutron Scattering, In-situ/operando Synchrotron and Neutron Experiments, Polymers, Thin Films, Battery, and Catalysis
[Resume]
2013-2018: Ph.D. Candidate, Department of Polymer Science, The University of Akron. Advisors: Dr. Mark D. Foster & Dr. Mark D. Soucek
2019-present: Postdoctoral Fellow at the Advanced Light Source, Lawrence Berkeley National Laboratory, Supervisor: Dr. Jinghua Guo
2020-present: Postdoctoral Fellow in Joint Center for Energy Storage Research (JCESR), a Department of Energy's Energy Innovation Hub.

Yi-Sheng Liu
Staff scientist in Sigray Inc.
E-mail: ysliu2@gmail.com
Main scientific activities: In-situ/operando X-ray spectroscopies, energy materials.
[Resume]
2006-2012: Ph.D. in Physics., Tamkang University, New Taipei City
2012-2013: Application Engineer, Grand Technology Inc., Hsinchu City
2013-2016: Postdoctoral Fellow, Advanced Light Source, Lawrence Berkeley National Laboratory
2016-2020: Project Beamline Scientist, Advanced Light Source, Lawrence Berkeley National Laboratory
2020-present: Staff scientist, Sigray Inc., Concord.

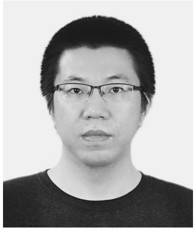

Xuefei Feng
University of Science and Technology of China, National Synchrotron Radiation Laboratory
E-mail: fengxf@ustc.edu.cn
Main scientific activities: Energy Sciences, Instrument Development for In-situ/Operando Synchrotron Radiation Experiments
[Resume]
2004-2008: Studies of Material Chemistry at the University of Science and Technology of China.
2008-2014: Studies of Synchrotron Radiation and Application at National Synchrotron Radiation Laboratory, University of Science and Technology of China.
2014-2016: Postdoctoral Fellow at the Shanghai Institute of Microsystem and Information Technology, Chinese Academy of Sciences.
2016-2019: Postdoctoral Fellow at the Advanced Light Source, Lawrence Berkeley National Laboratory.
2019-2021: Project Scientist at the Advanced Light Source, Lawrence Berkeley National Laboratory.
2021-present: Staff Scientist at National Synchrotron Radiation Laboratory, University of Science and Technology of China.

Per-Anders Glans
Beamline Scientist, Advanced Light Source, Lawrence Berkeley National Laboratory
E-mail: paglans@lbl.gov
Main scientific activities: Developing a high-resolution photon-in-photon-out experiment station at a new beamline.
[Resume]
1996, M. Sc. In Applied Physics and Electrical Engineering, Linkoping University, Linkoping, Sweden
2002, Ph.D. in Materials Science, Linkoping University, Linkoping, Sweden
2001-2007: Research Associate, Boston University
2007-2009: Research Associate, Advanced Light Source, Lawrence Berkeley National Laboratory
2009-2014: Scientific Engineering Associate, Advanced Light Source, Lawrence Berkeley National Laboratory
2014-present, Research Scientist, Advanced Light Source, Lawrence Berkeley National Laboratory

Jamie Nasiatka

Instrumentation Engineer, Advanced Light Source, Lawrence Berkeley National Laboratory
E-mail: jrnasiatka@lbl.gov

Main scientific activities: Development of high-stability precision positioning systems, Novel thermal management solutions for X-ray optics and synchrotron-based instrumentation

[Resume]

1989-1997: Staff Engineer at Argonne National Laboratory, High Energy Physics Division
1997-1998: Senior Engineer and department manager, Aerometrics Corporation
1998-2002: Senior Engineer, Nectar Therapeutic Systems
2003-present: Instrumentation Engineer, Advanced Light Source, Lawrence Berkeley National Laboratory

Dmitriy Voronov

Staff Scientist, Advanced Light Source, Lawrence Berkeley National Laboratory
E-mail: dlvoronov@lbl.gov

Main scientific activity: Material Science and Engineering, Nanofabrication, Development of Advanced X-ray Diffractive Optics, X-ray Multilayers, Multilayer Blazed Gratings.

[Resume]

1983-1989: Studies of Physics of Metals and Semiconductors at National Technical University, Ukraine.
1989-1997: Researcher at the Institute for Single Crystals, National Academy of Science of Ukraine.
1997-2007: X-ray Optics Laboratory, National Technical University, Ukraine.
2007-2011: Postdoctoral Researcher at the Advanced Light Source, Lawrence Berkeley National Laboratory.
2011-2014: Physicist Project Scientist at the Advanced Light Source, Lawrence Berkeley National Laboratory.
2014-present: Staff Scientist at the Advanced Light Source, Lawrence Berkeley National Laboratory.

Jun Feng

Professor of Department of Materials Science and Engineering, Institute for Quantum Science and Engineering, Southern University of Science and Technology, Shenzhen 518055, Guangdong, China,
E-mail: fengj@sustech.edu.cn

Research interests: Advanced material synthesis and characterization, Novel photocathode materials, High brightness electron beam, Ultrafast science, Quantum electron microscopy, Synchrotron radiation instrument and application.
Publication in refereed journals: ＞100

[Resume]

1982-1986: Studies of physics at Sichuan University, China.
1986-1991: Studies of physics and Doctoral thesis at the Institute of Modern Physics.
1991-1993: Postdoctoral Fellow at the Institute of Applied Physics.
1993-1995: Visiting Scientist at the Institute of Physical and Chemical Research, Japan.
1995-1998: Research Professor at the Institute of Applied Physics.
1998-2020: Staff Scientist at the Advanced Light Source, Lawrence Berkeley National Laboratory, USA.
2020-present, Professor of SusTech.

Yi-De Chuang

Staff Scientist, Advanced Light Source, Lawrence Berkeley National Laboratory
E-mail: ychuang@lbl.gov

Main scientific activity: Condensed Matter Physics, Synchrotron Instrumentation, Soft X-Ray Spectroscopies
Publication: ＞100, h-index 36

[Resume]

1990-1994: BS, Physics, National Taiwan University
1996-2001: PhD, Physics, University of Colorado at Boulder
2002-2006: Postdoctoral Researcher, Advanced Light Source, Lawrence Berkeley National Laboratory
2006-2015: Physicist Scientist, Advanced Light Source, Lawrence Berkeley National Laboratory
2015-present: Staff Scientist, Advanced Light Source, Lawrence Berkeley National Laboratory

Howard Padmore

Advanced Light Source, Lawrence Berkeley National Laboratory
E-mail: hapadmore@lbl.gov

Main scientific activities: material science using X-ray synchrotron techniques, Solid state physics of photocathodes and plasmonic devices, Diffractive X-ray imaging, and X-ray optics.

【Resume】

1977: B.Sc. in physics, Leicester University
1983: Ph.D., Leicester University, UK
1982-1988: Senior/Hier Scientific Officer, Surface Science Group, Daresbury
1989-1993: Principal Scientific Officer, Head Soft X-ray Group, Synchrotron Radiation Research Division, Daresbury Laboratory, UK
1993-present, Group leader for experimental systems, Advanced Light Source, Lawrence Berkeley National Laboratory
2005-present: Division Deputy, Advanced Light Source, Lawrence Berkeley National Laboratory
2018-present: Professor of Physics, Arizona State University.

Professional service and Honors:
1991-1994: Member of the editorial board of the (UK) Institute of Physics Journal of Measurement Science and Technology, J. Phys. E
1999-2008: Member of the editorial board of the Journal of Synchrotron Radiation
2008: Fellow Optical Society of America
2013: Fellow American Physical Society
2013: AVS Nerken Prize

Jinghua Guo

Senior Scientist and RIXS Program Lead, Advanced Light Source, Lawrence Berkeley National Laboratory
Adjunct Professor, Department of Chemistry and Biochemistry, University of California at Santa Cruz
Fellow of the American Physical Society
E-mail: jguo@lbl.gov

Research interests: In-situ / operando XAS, XES, and RIXS studies of energy storage, Controlled catalytic and chemical reactions, Development of in-situ/operando soft X-ray spectroscopy instrumentation and automation controls, Development of spatial-time-dependent RIXS, Development of Fourier transform interferometry instrumentation for XAS and RIXS

【Resume】

1985: B.Sc., Zhejiang University, China
1995: Ph.D. in physics at Uppsala University, Sweden
1995-1997: Postdoc at Uppsala University, Sweden
1997-2001: Assistant Professor, Department of Physics, Uppsala University, Sweden
2001-2004: Research Scientist, Advanced Light Source, Lawrence Berkeley National Laboratory
2004-2014: Staff Scientist, Advanced Light Source, Lawrence Berkeley National Laboratory
2012-present: Adjunct Professor, Department of Chemistry and Biochemistry, University of California, Santa Cruz
2014-present: Senior Scientist, Advanced Light Source, Lawrence Berkeley National Laboratory